

# Compatible Study on Utilizing Frequency for Non-Invasive Electrical Resistance Tomography Using COMSOL Multiphysics

Yasmin Abdul Wahab<sup>a</sup>, Ruzairi Abdul Rahim<sup>b\*</sup>, Mohd Hafiz Fazalul Rahiman<sup>c</sup>, Leow Pei Ling<sup>b</sup>, Suzanna Ridzuan Aw<sup>b</sup>, Fazlul Rahman Mohd Yunus<sup>b</sup>, Herlina Abdul Rahim<sup>b</sup>, Herman Wahid<sup>b</sup>, Shafishuhaza Sahlan<sup>b</sup>, Mohd Amri Md. Yunus<sup>b</sup>, Norhaliza Abdul Wahab<sup>b</sup>, Azian Abd Aziz@Ahmad<sup>b</sup>

<sup>a</sup>Department of Instrumentation & Control Engineering (ICE), Faculty of Electrical & Electronics Engineering, Universiti Malaysia Pahang, 26600, Pekan, Pahang, Malaysia

<sup>b</sup>Process Tomography and Instrumentation Engineering Research Group (PROTOM-i), Infocomm Research Alliance, Faculty of Electrical Engineering, Universiti Teknologi Malaysia, 81310 UTM Johor Bahru, Johor Malaysia

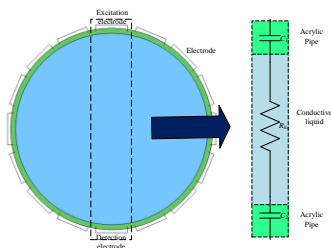
<sup>c</sup>Tomography Imaging Research Group, School of Mechatronic Engineering, Universiti Malaysia Perlis, 02600 Arau, Perlis, Malaysia

\*Corresponding author: ruzairi@fke.utm.my

## Article history

Received : 15 August 2014  
Received in revised form :  
5 January 2015  
Accepted : 10 February 2015

## Graphical abstract



## Abstract

Non-invasive techniques are widely applied in process plants compared to other sensing techniques. Due to advantages such as preventing corrosion to the sensor and lengthening the sensor lifespan, this technique is also applied in process tomography such as in non-invasive ERT system. The purpose of this paper is to investigate the compatibility of utilizing frequency for non-invasive ERT systems. Based on quasi-static electric fields, one pair of electrodes is used to simulate the optimum frequency for the system. It was firstly derived using a mathematical equation followed by simulation using finite element model software (COMSOL Multiphysics). Results showed that by simulating several frequencies to the system, a minimum frequency that should be applied is 2 MHz to ensure that the real part of the total impedance is dominant and also to neglect the reactance part of the total impedance for the non-invasive ERT system. Thus, the non-invasive ERT system is an alternative way for the industry in monitoring the performance of process plant.

**Keywords:** Non-invasive; ERT; COMSOL; quasi-static electric field; frequency

© 2015 Penerbit UTM Press. All rights reserved.

## 1.0 INTRODUCTION

Non-invasive and non-intrusive techniques are popular methods applied in the process tomography for chemical mixtures. The terms non-invasive and non-intrusive apply when sensors do not protrude into the vessel and are not directly in contact with the medium being measured [1]. In the past decade, the development of non-invasive techniques promises to be very significant for process plants and the chemical industries. Non-invasive methods benefit the industry more, compared to non-intrusive methods because of several advantages:

1. Decreasing the hazards of working with poisonous, radioactive, explosive, flammable or corrosive materials.
2. Assisting installation (and even retrofitting) and looking after the instruments even when the plant is on-stream.
3. Minimizing the safety and accountancy difficulties with valuable process materials.
4. Avoiding contamination of pure or sterile materials.

Indeed, the non-invasive method is one of the most favoured methods applied in process plants compared to other sensing techniques. There are several types of non-invasive process tomography implemented in chemical mixtures such as electrical capacitance tomography [2]–[7], ultrasonic tomography [8]–[20], x-ray computed tomography [21]–[26] and optical tomography [27]–[30]. Each type of process tomography has its own advantages and disadvantages.

However, in this paper, the authors are just focusing on electrical resistance tomography (ERT) research. The ERT reconstructs tomogram based on the conductivity distribution of the medium interested. The common technique implemented for ERT is invasive but still non-intrusive to the system such as in [31]–[38]. The main reason of applying the invasive technique is to make sure that there is a continuous contact between the electrodes and main fluids so that current can be conducted through the medium of interest [39]. The way in which the current technique is being measured can be done either by using the adjacent, opposite, boundary or diagonal methods [40].

Nevertheless, the current technique, namely, the ERT system, that comes into direct contact with the conductive liquid will cause corrosion to the ERT sensor and will inevitably limit the application and sensor lifespan.

In fact, B. Wang *et al.* [41]–[43] highlighted this issue and proposed a non-invasive ERT system for chemical mixtures. The capacitively coupled contactless conductivity detection (C<sup>4</sup>D) was introduced by the group and it was proven that it can be used for a non-invasive ERT system. Using this particular research as a springboard, this paper aims to investigate and proof a suitable utilizing frequency that can be used for non-invasive ERT systems.

## ■2.0 QUASI-STATIC ELECTRIC FIELD FOR NON-INVASIVE ERT SYSTEM

Electrical tomography techniques apply the knowledge of electromagnetic fields based on Maxwell's equations to describe the electromagnetic phenomena. Subjected to Maxwell's equations, it will determine the state of the medium, whether electrostatic field, magnetostatic field, electromagnetic field or quasi-static field; depending on the field interested and the medium considered. However, the common frequency used in the electrical tomography to execute the electrical field in the sensing region is up to the order of 1 MHz [44].

Based on the electromagnetic spectrum, the frequency range is still small compared to microwave, infrared and other frequencies. Thus, it will cause a large wavelength of electromagnetic radiation compared to the physical dimension of the system. The physical dimension in the electrical tomography referred to is the typical diameter of sensor system (range between 1 cm and 1 m) [44]. As a result, the wavelength will go beyond the sensor size by several orders of magnitude. This means that the system field is propagated instantaneously. Consequently, the electromagnetic field can be treated as a quasi-static approximation [45].

The quasi-static approximation can be divided into two conditions, namely, electro quasi-static (EQS) and magneto quasi-static (MQS) [46]. In EQS, the magnetic induction is neglected, resulting in the system being influenced by the capacitive effect. Meanwhile, MQS is only influenced by the inductive effect, and the displacement current is neglected. Since the non-invasive ERT only considers conductivity distribution, the EQS has been applied for the system. Hence, the Maxwell equations for EQS are represented as follows:

$$\nabla \cdot \mathbf{D} = \rho \quad (\text{Gauss law}) \quad (1)$$

$$\nabla \cdot \mathbf{B} = 0 \quad (\text{Gauss law}) \quad (2)$$

$$\nabla \times \mathbf{H} = \mathbf{J} + j\omega \mathbf{D} \quad (\text{Ampere's Law}) \quad (3)$$

$$\nabla \times \mathbf{E} = 0 \quad (4)$$

where  $\mathbf{D}$  is the electric flux density;  $\mathbf{E}$  is the electric field intensity,  $\mathbf{J}$  is the current density and  $\rho$  is the free charge density.  $\mathbf{B}$  is the magnetic flux density;  $\mathbf{H}$  is the magnetic field intensity and  $\omega$  is the angular frequency. Additionally, the relationship between  $\mathbf{D}$  and  $\mathbf{E}$ ,  $\mathbf{J}$  and  $\mathbf{E}$  can be represented as follows:

$$\mathbf{D} = \epsilon \mathbf{E} \quad (5)$$

$$\mathbf{J} = \sigma \mathbf{E} \quad (6)$$

The non-invasive ERT considers the voltage as the excitation signal and current as the detection signal. So, it is important to know the sensing field principle in the system and also how the

current signal is propagated and measured at the detection electrode. Based on Equation (3), if the equation is multiplied with divergence of each side, it becomes:

$$\nabla \cdot \nabla \times \mathbf{H} = \nabla \cdot \mathbf{J} + \nabla \cdot j\omega \mathbf{D} \quad (7)$$

Since, the divergence of the curl is identically zero; thus, Equation (7) is simplified and becomes an equation of continuity [45] as in Equation (8).

$$0 = \nabla \cdot \mathbf{J} + \nabla \cdot j\omega \mathbf{D} \quad (8)$$

Knowing that the potential gradient,  $\mathbf{E} = -\nabla V$  [47], where  $V$  is the potential distribution, and substituting Equation (5), (6) and  $\mathbf{E}$  into (8), resulting in the EQS equation of sensing field in the non-invasive ERT system to be shown in Equation (9):

$$\nabla \cdot (\sigma + j\omega \epsilon) \nabla V = 0 \quad (9)$$

Based on Equation (9), it is clearly seen that the non-invasive ERT is based on the  $\sigma$  and  $\epsilon$  due to the conductive medium and insulating pipe implemented. Here, the main reason for the need of EQS in the sensing field is due to the need of the current to flow through the two different mediums.

Likewise, Equation (9) is also known as Poisson-type differential equation. The specific sensing field of non-invasive ERT system in two dimensions is determined by the following Equation (10):

$$\left\{ \begin{array}{ll} \nabla \cdot (\sigma(x, y) + j\omega \epsilon(x, y)) \nabla V(x, y) = 0 & (x, y) \subseteq \Omega \\ V_i(x, y) = V_0 & (x, y) \subseteq \Gamma_i \\ V_j(x, y) = 0 & (x, y) \subseteq \Gamma_j \\ \frac{dV(x, y)}{dn} = 0 & (x, y) \subseteq \Gamma_k, (k \neq i, j) \end{array} \right. \quad (10)$$

The  $\Gamma_i$  and  $\Gamma_j$  represent the spatial locations of  $n$  electrodes;  $i$  and  $j$  are the indexes of excitation and detection electrodes respectively, and  $V_0$  is the applied voltage to the system.

The modeling to proof the concept is done and analyzed by Finite Element Model (FEM) using FEM simulation software COMSOL Multiphysics. Based on the simulation, the current value between each pair of electrode can be obtained from Ampere's Law in Equation (3) which is totally different compared to [42]. Based on Ampere's law, by considering the integral form; the total current equation on the surface of the sensing field can be obtained based on Equation (11) [48]:

$$\oint_c \mathbf{H} \, dl = \oint_s \mathbf{J} \, ds + \oint_s \frac{d}{dt} \mathbf{D} \, ds = I_c + I_d = I \quad (11)$$

Where  $I$  is the total current on the surface,  $I_c$  is conduction current, and  $I_d$  is a displacement current. The  $S$  is the surface of the electrode, and  $dS$  is the discrete element of the electrode. At a later stage, by implementing a high enough frequency to the system, the reactance part of the impedance can be ignored. So, the resistance between any pairs of electrode can be determined by Ohm's law such as in (12). The  $R_{i,j}$ ,  $V_0$  and  $I_{i,j}$  are referred to as the resistance, voltage and current for every pair of electrode respectively.

$$R_{i,j} = \text{real} \frac{V_0}{I_{i,j}} \tag{12}$$

### 3.0 NON-INVASIVE ERT SENSOR

As mentioned in B. Wang *et al.* [41]-[42], the idea of implementing the non-invasive ERT system is based on applications used in analytical chemical applications. The non-invasive ERT system in two dimensions could be represented as in Figure 1.

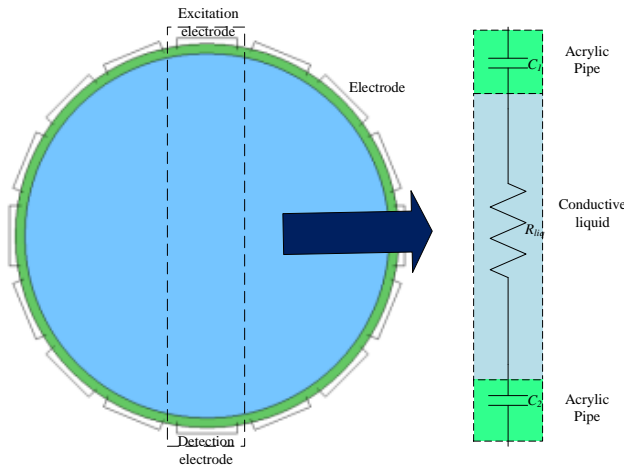


Figure 1 Non-invasive ERT system

According to Figure 1, since all the pairing of electrodes are similar, only one pair of electrode is needed to make a simple calculation and prove the suitable frequency for non-invasive ERT systems. By assuming the electrode and the conductive liquid as a coupling capacitance and the conductive liquid as a resistance, the conductivity of the medium can be obtained based on the resistance. The resistance can be measured based on the total impedance when the reactance can be neglected due to the high enough frequency applied to the system. A simple calculation can thus be obtained based on Equation (13).

$$Z_T = R_{liq} - j \frac{1}{2\pi f \left( \frac{C_1 C_2}{C_1 + C_2} \right)} \tag{13}$$

The  $Z_T$  is the total impedance of the sensing field for one pair of electrode measurement;  $R_{liq}$  is the resistance of conductive liquid, and  $C_1$  and  $C_2$  are the coupling capacitances between the electrode and the conductive liquid.

Moreover, the electrical properties of the insulating pipe and the conductive liquid should be considered. Here, based on the quasi-static electric field as shown in Equation (10), only electrical permittivity and electrical conductivity are considered. Consequently, the capacitance,  $C$  and the resistance,  $R$  values can be measured by using Equation (14) [49] and (15) [50].

$$R = \frac{L}{\sigma A} \ (\Omega) \tag{14}$$

$$C = \frac{\epsilon_0 \epsilon_r A}{d} \ (\text{F}) \tag{15}$$

where  $L$  is the inner diameter of the insulating pipe,  $\sigma$  is the electrical conductivity of the conductive liquid,  $A$  is the area of electrode,  $\epsilon_0$  is the permittivity of free space,  $\epsilon_r$  is the relative permittivity of insulating pipe, and  $d$  is the thickness of the insulating pipe.

Let's say, if the authors use 16 rectangular copper electrodes where the area of each electrode is approximately  $2.66 \times 10^{-3} \text{ m}^2$ , acrylic pipe with thickness 3 mm and inner diameter 104 mm,  $\sigma$  is  $5 \times 10^{-3} \text{ S/m}$ , and  $\epsilon_r$  is 3.45; by using Equation (14) and (15), the resistance value of the conductive liquid and the capacitance value for each of the coupling capacitance will be around 7.81 k $\Omega$  and 27.11 pF respectively. Hence, based on Equation (13), a minimum frequency that should be applied is 2 MHz in ensuring the real part of the total impedance is dominant and also to neglect the reactance part of the total impedance for the non-invasive ERT system. This means that, if the frequency is below 2 MHz, the conductivity of the non-invasive ERT system cannot be determined because of the existent of the reactance part. Later, the value of the current flow through the medium can be measured. A simple schematic diagram of the circuits for one pair of electrode can be shown in Figure 2.

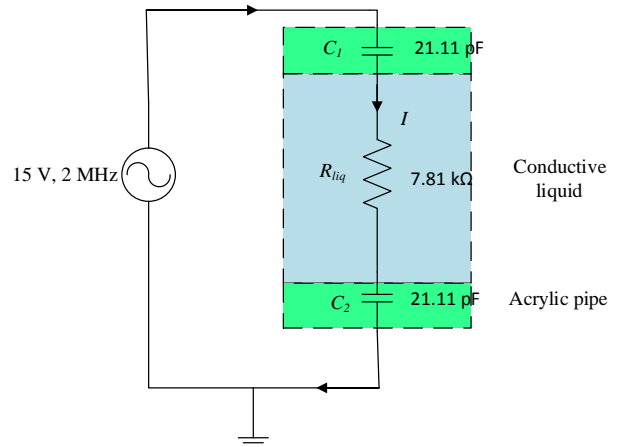


Figure 2 Schematic diagram for one pair of electrode measurement

Value of the current can be calculated based on Ohm's law. If the voltage applied at the excitation electrode is 15 V with frequency 2 MHz and the authors assumed the reactance part is neglected, the value of current at the detection electrode should be around 2 mA. The current value flow through the non-invasive ERT system should be the same because the system is assumed in RC series connection. Later, this concept was proven using COMSOL Multiphysics software with several frequencies to analyze whether the electricity can penetrate and distribute evenly spaced through the acrylic pipe and conductive liquid or not.

### 4.0 SIMULATION AND ANALYSIS OF MODEL

In COMSOL Multiphysics software, the process of designing the model can be divided into the following:

1. The geometry in two dimensions is drawn according to the specific dimensions as shown in Table 1 and Figure 3(a).

2. The material for each of the domains has been defined.
3. The frequency domain solver in electric current module has been selected since the system is a quasi-static electric field. A suitable frequency has been set and frequency user defined.
4. For the boundary setting, the boundary conditions for excitation electrode has been set to electric potential and grounded for detection electrode.
5. The mesh for system has been generated. See Figure 3(b).
6. Finally, the study has been computed to get results, and the capabilities of post-processing in COMSOL applied to calculating the current and voltage. Different points between the excitation electrode (point 1) and the detection electrode (point 15) investigated are shown in Figure 3(c).

**Table 1** Properties and specific dimension

No	Item	Dimension
1	Electrode width	17.76 mm
2	Electrode length	150 mm
3	Thickness of pipe	3 mm
4	Inner diameter of the pipe	104 mm
5	Electrical Permittivity	$\epsilon_r = 3.45$ (acrylic) $\epsilon_r = 80$ (water)
6	Electrical Conductivity	$\sigma = 3 \times 10^{-14}$ S/m (acrylic) $\sigma = 5 \times 10^{-3}$ S/m (water)

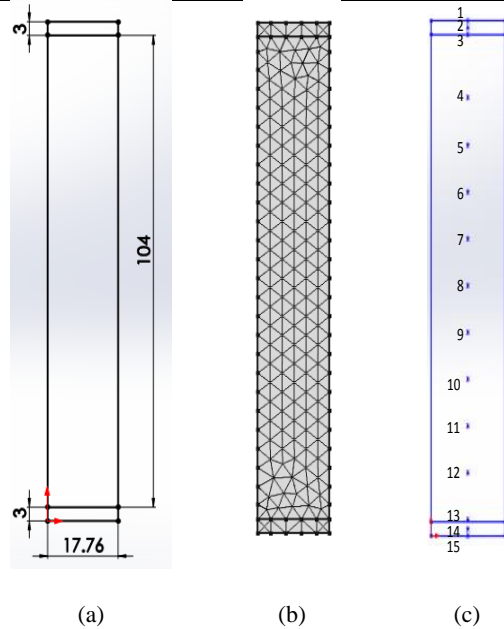


**Figure 3** (a) Illustration of one pair of electrode of non-invasive ERT (all units are in mm); (b) Finer FEM meshing; (c) The location of point 1 till point 15 measured

As explained in Section 3, the top of the rectangular was set as the exciting electrode with electrical potential 15 V and the bottom part set as the ground. The frequency applied to the system was 2 MHz. The simulation is to investigate whether the signal given at the excitation electrode can penetrate through the acrylic pipe or not. As calculated in Section 3, if the frequency applied is high enough, the voltage signal should penetrate

through the acrylic pipe and drop gradually to the detection electrode. This is because the electrode detected is connected to the ground, and later the current can be measured at the detection electrode. As the system is assumed to be the RC series circuit, the current flow from the excitation electrode to the detection electrode should be the same. Thus, the best method to investigate the way of signal propagation is based on the voltage distribution. Moreover, based on Ohm’s law, the voltage is proportional to the current. Thus, it is not a big issue if the voltage distribution is considered in identifying the suitability of utilizing frequency for a non-invasive ERT system, even though the main concern for the non-invasive ERT is the value of the current. As a result, the voltage distribution decreases significantly from top to the ground with the frequency of 2 MHz as illustrated in Figure 5. This value is significant with the calculated value. Correspondingly, there was a very poor voltage distribution in 4(a) which decreased sharply from 15 V to around 7 V and remained constant in the conductive liquid. Similar to 4(b) and (c), even though the way of the voltage signal propagation is improved, it was observed that the signal did not significantly drop compared to Figure 4(d).

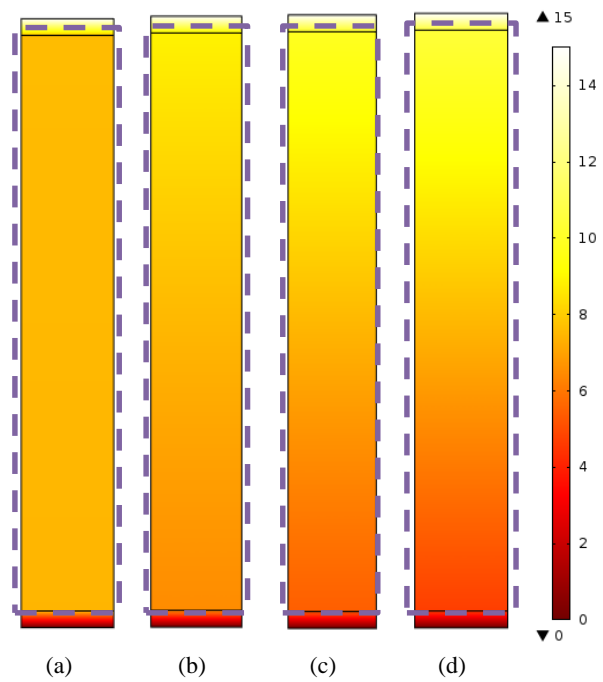


**Figure 4** Voltage distribution with different frequencies for (a) 100 kHz, (b) 500 kHz, (c) 1 MHz, and (d) 2 MHz

Besides, the voltage distribution in the medium was also analyzed in the line graph by taking 15 points from the top to the bottom part as shown in 5. Points 1 and 15 are the locations between the excitation electrode and the detection electrode respectively; points 2 and 14 are in the acrylic pipe, and points 3 till 13 are the points in the conductive liquid as illustrated in Figure 4(c). There was a noticeable drop in the voltage distribution for all frequencies applied. Despite the voltage distribution decreasing steadily to the ground at points 3 to 13 when the frequency applied increased, It could infer from this figure that, 2 MHz was the minimum frequency to be applied for the electricity to penetrate through the acrylic pipe for the non-invasive ERT system to work properly.

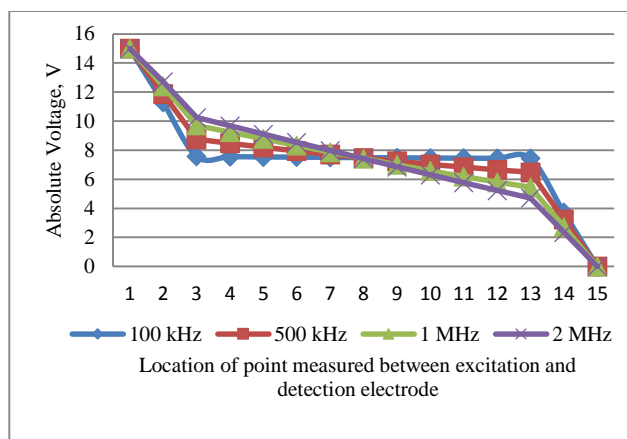


**Figure 5** Absolute voltage versus location of fifteen points measured from excitation electrode (point 1) to the detection electrode (point 15)

## 5.0 CONCLUSION

In short, the objective of this paper has been achieved. The non-invasive ERT system can indeed be applied to determine the conductivity of the interest medium if the frequency used is high enough, i.e., 2 MHz for acrylic pipe with an outer diameter of 110 mm and thickness of 3 mm. Different materials of insulating pipe and conductive liquid implemented will need different frequencies to make the system work properly. Moreover, it is assumed that the non-invasive ERT system will need an MHz frequency instead of just a kHz frequency to be applied to the system for industry application because of the quasi-static electric field condition. Nevertheless, it should be noted that this research work is a preliminary study. Thus, further studies could be done in the future to optimize the sensor design for non-invasive ERT systems in terms of the width of the electrode, thickness of the pipe and even the length of the electrode. Finally, it is believed that further investigations and upgrading of the ERT systems will provide wide-ranging alternatives in visualizing and monitoring chemical mixtures, which could assist in improving the performance of process plants.

## Acknowledgement

The authors would like to thank the Ministry of Higher Education and Universiti Malaysia Pahang for funding the study. Special appreciation also goes to Universiti Teknologi Malaysia and the PROTOM research group for their unwavering support and invaluable assistance.

## References

- [1] R. C. Asher. 1983. Ultrasonic Sensors in the Chemical and Process Industries. *J. Phys. E.* 6(10): 959–963.
- [2] R. Banasiak, R. Wajman, T. Jaworski, P. Fiderek, H. Fidos, J. Nowakowski, and D. Sankowski. 2014. Study on Two-phase Flow Regime Visualization and Identification Using 3D Electrical Capacitance Tomography and Fuzzy-logic Classification. *Int. J. Multiph. Flow.* 58: 1–14.
- [3] R. Zhang, Q. Wang, H. Wang, M. Zhang, and H. Li. 2014. Data Fusion in Dual-mode Tomography for Imaging Oil–gas Two-phase Flow. *Flow Meas. Instrum.* 37: 1–11.
- [4] Y. Zhao, H. Yeung, E. E. Zorgani, A. E. Archibong, and L. Lao. 2013. High Viscosity Effects on Characteristics of Oil and Gas Two-phase Flow in Horizontal Pipes. *Chem. Eng. Sci.* 95: 343–352.

- [5] E. J. Mohamad, R. Abdul Rahim, P. L. Leow, M. H. Fazalul Rahiman, O. M. F. Marwah, and N. M. Nor Ayob. 2012. Segmented Capacitance Tomography Electrodes: A Design and Experimental Verifications. *IEEE Sens. J.* 12(5): 1589–1598.
- [6] R. Yan, C. Pradeep, J. Muwanga, and S. Mylvaganam. 2012. Interface imaging in multiphase flow based on frame by frame eigenvalues of capacitance matrices from Electrical Capacitance Tomographic systems. In *IEEE International Conference on Imaging Systems and Techniques.* 2, pp. 466–469.
- [7] W. A. Al-Masry, E. M. Ali, S. A. Alshebeili, and F. M. Mousa. 2010. Non-invasive Imaging of Shallow Bubble Columns Using Electrical Capacitance Tomography. *J. Saudi Chem. Soc.* 14(3): 269–280.
- [8] J. Abbaszadeh, H. Abdul Rahim, R. Abdul Rahim, and S. Sarafi. 2014. Frequency Analysis of Ultrasonic Wave Propagation on Metal Pipe in Ultrasonic Tomography System. *Sens. Rev.* 34(1): 13–23.
- [9] M. H. F. Rahiman, R. A. Rahim, H. A. Rahim, E. J. Mohamad, Z. Zakaria, and S. Z. M. Muji. 2014. An Investigation on Chemical Bubble Column Using Ultrasonic Tomography for Imaging of Gas Profiles. *Sensors Actuators B Chem.* 202: 46–52.
- [10] F. R. Mohd Yunus, N. A. Noor Azlan, N. M. Nor Ayob, M. J. Puspanathan, M. F. Jumaah, C. L. Goh, R. Abdul Rahim, A. Ahmad, Y. Md Yunus, and H. Abdul Rahim. 2013. Simulation Study of Bubble Detection Using Dual-Mode Electrical Resistance and Ultrasonic Transmission Tomography for Two-Phase Liquid and Gas. *Sensors & Transducer.* 150(3): 97–105.
- [11] M. J. Puspanathan, N. M. Nor Ayob, Fazlul Rahman Yunus, Khairul Hamimah Abas, H. Abdul Rahim, P. L. Leow, R. Abdul Rahim, F. A. Phang, M. H. Fazalul Rahiman, and Z. Zakaria. 2013. Ultrasonic Tomography Imaging for Liquid-Gas Flow Measurement. *Sensors & Transducer.* 148(1): 33–39.
- [12] M. H. F. Rahiman, R. A. Rahim, H. A. Rahim, N. M. N. Ayob, E. J. Mohamad, and Z. Zakaria. 2013. Modelling Ultrasonic Sensor for Gas Bubble Profiles Characterization of Chemical Column. *Sensors Actuators B Chem.* 184: 100–105.
- [13] J. Abbaszadeh, H. Abdul Rahim, R. Abdul Rahim, S. Sarafi, M. Nor Ayob, and M. Faramarzi. 2013. Design Procedure of Ultrasonic Tomography System with Steel Pipe Conveyor. *Sensors Actuators A Phys.* 203: 215–224.
- [14] N. M. Nor Ayob, M. J. Puspanathan, R. Abdul Rahim, M. H. Fazalul Rahiman, F. R. Mohd Yunus, S. Buyamin, I. M. Abd Rahim, and Y. Md. Yunus. 2013. Design Consideration for Front-End System in Ultrasonic Tomography. *J. Teknol.* 64(5): 53–58.
- [15] M. H. Fazalul Rahiman, R. Abdul Rahim, H. Abdul Rahim, and N. M. Nor Ayob. 2012. Novel Adjacent Criterion Method for Improving Ultrasonic Imaging Spatial Resolution. *IEEE Sens. J.* 12(6): 1746–1747.
- [16] Y. Murai, Y. Tasaka, Y. Nambu, Y. Takeda, and S. R. Gonzalez A. 2010. Ultrasonic Detection of Moving Interfaces in Gas–liquid Two-phase Flow. *Flow Meas. Instrum.* 21(3): 356–366.
- [17] N. M. Nor Ayob, M. H. Fazalul Rahiman, Z. Zakaria, S. Yaacob, R. Abdul Rahim, and M. R. Manan. 2011. Simulative study in liquid/Gas Two-Phase Flow Measurement for Dual-Plane Ultrasonic Transmission-Mode Tomography. *J. Teknol.* 54: 79–94.
- [18] J. Puspanathan, R. Abdul Rahim, and M. H. Fazalul Rahiman. 2011. Ultrasonic Tomography System in Liquid-Gas Flow Monitoring. *J. Teknol.* 54: 255–266.
- [19] N. M. Nor Ayob, S. Yaacob, Z. Zakaria, M. H. Fazalul Rahiman, R. Abdul Rahim, and M. R. Manan. 2010. Improving Gas Component Detection of an Ultrasonic Tomography System for Monitoring Liquid/Gas Flow. In *2010 6th International Colloquium on Signal Processing & its Applications.* 1(1): 1–5.
- [20] Z. Zakaria, M. H. Fazalul Rahiman, and R. Abdul Rahim. 2010. Simulation of the Two-Phase Liquid–Gas Flow through Ultrasonic Transceivers Application in Ultrasonic Tomography. *Sensors & Transducer.* 112(1): 24–38.
- [21] Z. Zhang, M. Bieberle, F. Barthel, L. Szalinski, and U. Hampel. 2013. Investigation of Upward Cocurrent Gas–liquid Pipe Flow Using Ultrafast X-Ray Tomography and Wire-Mesh. *Flow Meas. Instrum.* 32: 111–118.
- [22] S. Boden, M. Bieberle, and U. Hampel. 2008. Quantitative Measurement of Gas Hold-up Distribution in a Stirred Chemical Reactor Using X-Ray Cone-beam Computed Tomography. *Chem. Eng. J.* 139(2): 351–362.
- [23] T. J. Heindel, J. N. Gray, and T. C. Jensen. 2008. An X-ray System for Visualizing Fluid Flows. *Flow Meas. Instrum.* 19: 67–78.
- [24] C. Wu, Y. Cheng, Y. Ding, F. Wei, and Y. Jin. 2007. A novel X-ray Computed Tomography Method for Fast Measurement of Multiphase Flow. *Chem. Eng. Sci.* 62: 4325–4335.
- [25] H. Prasser, M. Misawa, and I. Tiseanu. 2005. Comparison between Wire-mesh Sensor and Ultra-fast X-Ray Tomograph for an Air–Water Flow in a Vertical Pipe. *Flow Meas. Instrum.* 16: 73–83.

- [26] J. L. Hubers, A. C. Striegel, T. J. Heindel, J. N. Gray, and T. C. Jensen. 2005. X-ray Computed Tomography in Large Bubble Columns. *Chem. Eng. Sci.* 60: 6124–6133.
- [27] N. S. Mohd Fadzil, R. Abdul Rahim, M. S. Karis, S. Z. Mohd Muji, M. F. Abdul Sahib, M. S. B. Mansor, N. M. Nor Ayob, M. F. Jumaah, and M. Z. Zawahir. 2013. Hardware Design of Laser Optical Tomography System for Detection of Bubbles Column. *J. Teknol.* 64(5): 69–73.
- [28] S. Ibrahim, M. A. M. Yunus, R. G. Green, and K. Dutton. 2012. Concentration Measurements of Bubbles in a Water Column Using an Optical Tomography System. *ISA Trans.* 51(6): 821–826.
- [29] E. Schleicher, M. J. Da Silva, S. Thiele, A. Li, E. Wollrab, and U. Hampel. 2008. Design of an Optical Tomograph for the Investigation of Single- and Two-phase Pipe Flows. *Meas. Sci. Technol.* 19(9): 094006.
- [30] Y. Md. Yunus, R. Abdul Rahim, and R. G. Green. 2008. Initial Result on Measurement of Gas Volumetric Flow Rate in Gas / Liquid Mixtures using Linear CCD. *J. Teknol.* 48(D): 1–11.
- [31] W. Yenjaichon, J. R. Grace, C. Jim Lim, and C. P. J. Bennington. 2013. Characterisation of Gas Mixing in Water and Pulp-suspension Flow Based on Electrical Resistance Tomography. *Chem. Eng. J.* 214: 285–297.
- [32] M. Sobri, A. Ahmad, M. Irwan, and S. Jantan. 2013. ERT Visualization of Gas Dispersion Performance of Aerofoil and Radial Impellers in an Agitated Vessel. *J. Teknol.* 64(5): 75–78.
- [33] A. D. Okonkwo, M. Wang, and B. Azzopardi. 2013. Characterisation of a High Concentration Ionic Bubble Column Using Electrical Resistance Tomography. *Flow Meas. Instrum.* 31: 69–76.
- [34] C. Yang, H. Wang, and Z. Cui. 2012. Application of Electrical Resistance Tomography in Bubble Columns for Volume Fraction Measurement. In *IEEE International Conference on Instrumentation and Measurement Technology (I2MTC 2012)*. 60820106002. 1199–1203.
- [35] J. Kourunen, T. Niitti, and L. M. Heikkinen. 2011. Application of Three-dimensional Electrical Resistance Tomography to Characterize Gas Holdup Distribution in Laboratory Flotation Cell. *Miner. Eng.* 24(15): 1677–1686.
- [36] X. Deng, G. Li, Z. Wei, Z. Yan, and W. Yang. 2011. Theoretical Study of Vertical Slug Flow Measurement by Data Fusion From Electromagnetic Flowmeter and Electrical Resistance Tomography. *Flow Meas. Instrum.* 22(4): 272–278.
- [37] H. Jin, S. Yang, G. He, M. Wang, and R. A. Williams. 2010. The Effect of Gas-liquid Counter-current Operation on Gas Hold-up in Bubble Columns Using Electrical Resistance Tomography. *J. Chem. Technol. Biotechnol.* 85(9): 1278–1283.
- [38] Y. Xu, H. Wang, Z. Cui, and F. Dong. 2009. Application of Electrical Resistance Tomography for Slug Flow Measurement in Gas-liquid Flow of Horizontal Pipe. In *IEEE International Workshop on Imaging Systems and Techniques (IST 2009)*. 319–323.
- [39] M. Sharifi and B. Young. 2013. Electrical Resistance Tomography (ERT) applications to Chemical Engineering. *Chem. Eng. Res. Des.* 91(9): 1625–1645.
- [40] F. Dickin and M. Wang. 1996. Electrical Resistance Tomography for Process Applications. *Meas. Sci. Technol.* 7(3): 247–260.
- [41] B. Wang, Y. Hu, H. Ji, Z. Huang, and H. Li. 2013. A Novel Electrical Resistance Tomography System Based on C 4 D Technique. *IEEE Trans. Instrum. Meas.* 62(5): 1017–1024.
- [42] B. Wang, W. Zhang, Z. Huang, H. Ji, and H. Li. 2013. Modeling and Optimal Design of Sensor for Capacitively Coupled Electrical Resistance Tomography System. *Flow Meas. Instrum.* 31: 3–9.
- [43] B. Wang, Y. Hu, H. Ji, Z. Huang, and H. Li. 2012. A Novel Electrical Resistance Tomography System Based on C4D Technique. In *IEEE International Conference on Instrumentation and Measurement Technology (I2MTC 2012)*. 1929–1932.
- [44] Z. Cao, L. Xu, C. Xu, and H. Wang. 2010. Electrical Resistance Tomography(ERT) by using an ECT Sensor. In *IEEE International Conference on Imaging Systems and Techniques (IST 2010)*. 63–66.
- [45] J. Larsson. 2006. Electromagnetics from a Quasistatic Perspective. *Am. J. Phys.* 75(3): 230.
- [46] D. K. Kalluri. 2013. *Principles of Electromagnetic Waves And Materials*. FL. : CRC Press. 11–16.
- [47] J. William H.Hayt and John A. Buck. 2006. Energy and Potential. In *Engineering Electromagnetics*. 99.
- [48] F. T. Ulaby, E. Michielssen, and U. Ravaioli. 2010. *Fundamentals of Applied Electromagnetics*. 6th ed. Boston : Prentice Hall. 299–300.
- [49] C. Kuo-Sheng, D. Isaacson, J. C. Newell, and D. G. Gisser. 1989. Electrode Models for Electric Current Computed. *IEEE Trans. Biomed. Eng.* 36(9): 918–924.
- [50] M. A. Zimam, E. J. Mohamad, R. Abdul Rahim, and L. P. Leow. 2011. Sensor Modeling for Electrical Capacitance Tomography System using COMSOL Multiphysics. *J. Teknol.* 55(2): 33–47.